Electronic Supplementary Material (ESI) for ChemComm.

Self-assembled hole-transporting material constructed by chlorination and conjugation strategies toward the efficient organic solar cells

Xinjie Zhou,[a] Renyong Geng,[c*] Shanlei Xu,[a] Xingting Liu, [a] Yahui Yang,[a] Shenzheng Gao, [a] Hao Xu, [a] Weiguo Zhu, [a] and Xin Song, [a,b*]

a: School of Materials Science and Engineering, Jiangsu Engineering Laboratory of Light-Electricity-Heat Energy-Converting Materials and Applications, Changzhou University, Changzhou 213164, P. R. China

b: Key Laboratory of Advanced Energy Materials Chemistry (Ministry of Education), Nankai University, Tianjin 300071, P. R. China

c: School of Chemistry and Materials Engineering, Fuyang Normal University, Fuyang, 236037, P. R. China.

*Correspondence: xin.song@cczu.edu.cn, renyonggeng@fynu.edu.cn

1. Materials

D18 and PNDI-F3N-Br was purchased from Nanjing Zhiyan Inc. LTD. N3 was purchased from Dethon Optoelectronics Materials Inc. LTD. L8-BO were purchased from Nanjing Zhiyan. Poly(3,4-ethylenedioxythiophene):poly(styrenesulfonate) (PEDOT:PSS) PEDOT:PSS, Baytron P VP Al 4083 from H. C. Starck was commercially available from Heraeus (Germany). Ag was purchased from ZhongNuo

Advanced Material（Beijing）Technology Co., Ltd. All materials and solvents were commercially available and used as received.

2. Devices Fabrication

The devices were fabricated with conventional structures of ITO/HTL/BHJ/PNDI-F3N-Br/Ag(100 nm). The patterned ITO glass substrates (SuZhou ShangYang Solar Technology Co., Ltd.) were cleaned sequentially under sonication with deionized water and isopropanol, and then dried at 60 ℃ in a baking oven overnight. After 10 s plasma treatment (LEBO Science, PT500, 750 W), a PEDOT:PSS layer (~30 nm) was spin-coated on ITO substrate at 4800 rpm for 30 s, and then baked in air at 150 °C for 15 min; Sequentially, the active layer solution of D18:N3 (1:1.6, chloroform, 10 mg/ml) was spin-coated at 3000 rpm for 30 s. For TPA-CN-COOH HTL, 2Cl-TPA-CN-COOH was firstly dissolved in ethanol solvent with a concentration of 0.3 mg/ml. After 4 hours stirring at room temperature, this 2Cl-TPA-CN-COOH solution was coated on top of ITO substrate with varied spin speed and thermal annealing. Then the D18:N3 solution is deposited on top of 2Cl-TPA-CN-COOH substrate. The preparation of TPA-CN-COOH is similar to that of 2Cl-TPA-CN-COOH, where TPA-CN-COOH was firstly dissolved in ethanol solvent with a concentration of 0.3 mg/ml. After 4 hours stirring at room temperature, this TPA-CN-COOH solution was coated on top of ITO substrate with spin speed (4000 rpm) and thermal annealing treatment (100 ^{o}C, 5 min). Then the D18:N3 solution is deposited on top of 2Cl-TPA-CN-COOH substrate. After that, PFNDI-F3N-Br methanol solution with a concentration of 0.5 mg mL^{-1} was spin-coated on the active layer at 2000 rpm for 30 s. To complete the fabrication of the devices, 100

nm of Ag is thermally evaporated through a mask under a vacuum of ~5 × 10^{-4} mbar. The active area of the devices was 0.06 cm^2.

3. Device characterizations

***J-V* and EQE**

The photovoltaic performance was measured under an AM 1.5G spectrum from a solar simulator (Newport) with an active are of 0.06 cm^2. The illuminated are with a mask is 0.568 cm^2. The current density-voltage (J-V) characteristics were recorded with a Keithley 2400 source meter with a range from −0.2 to 1.2 V with a scan step of 50 mV and a dwell time of 10 ms. The light intensity of the light source was calibrated before the testing by using a standard silicon (Si) solar cell, as calibrated by a National Renewable Energy Laboratory (NREL) certified silicon photodiode, giving a value of 100 mW/cm^2. The external quantum efficiency (EQE) spectra were obtained on a commercial EQE measurement system (Taiwan, Enlitech, QE-R3011). The light intensity at each wavelength was calibrated by a standard single-crystal Si photovoltaic cell.

The transient photoelectronic test was measured by Piaos system (Switzerland).

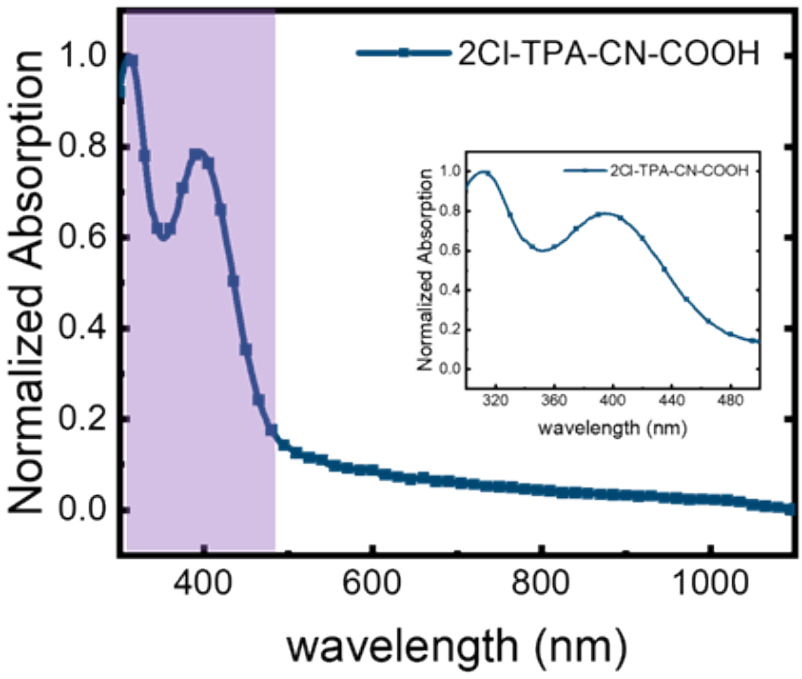

Figure S1. The absorption spectrum of 2Cl-TPA-CN-COOH. And the enlarged image is the absorption curve of 2Cl-TPA-CN-COOH at 300-500 nm.

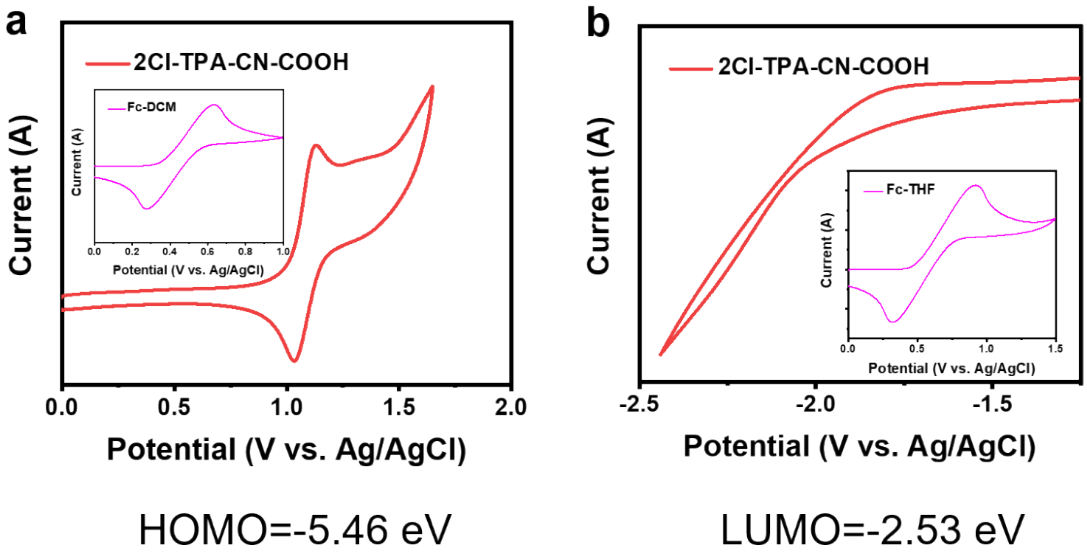

Figure S2. CV curves of 2Cl-TPA-CN-COOH with ferrocene (Fc/Fc+) as the external standard. Cyclic voltammetry (CV) techniques were conducted to evaluate the electrochemical properties of 2Cl-TPA-CN-COOH. The HOMO and LUMO energy levels are calculated from onset oxidation and reduction potentials with the calibration by ferrocene/ferrocenium. (a) The oxidation potential is tested in CH_2Cl_2 solution, while (b) reduction potential is in THF solution.

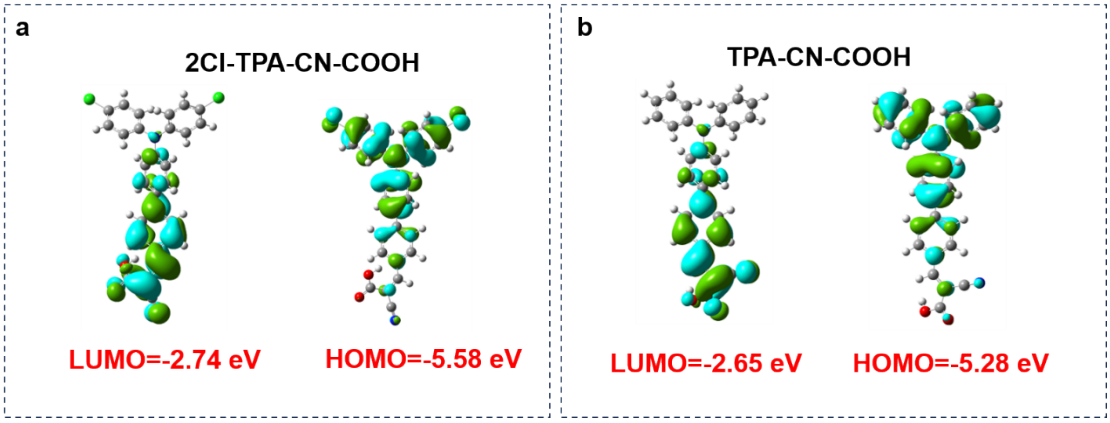

Figure S3. The calculated LUMO and HOMO level of 2Cl-TPA-CN-COOH and TPA-CN-COOH based on the molecular density function theory simulation.

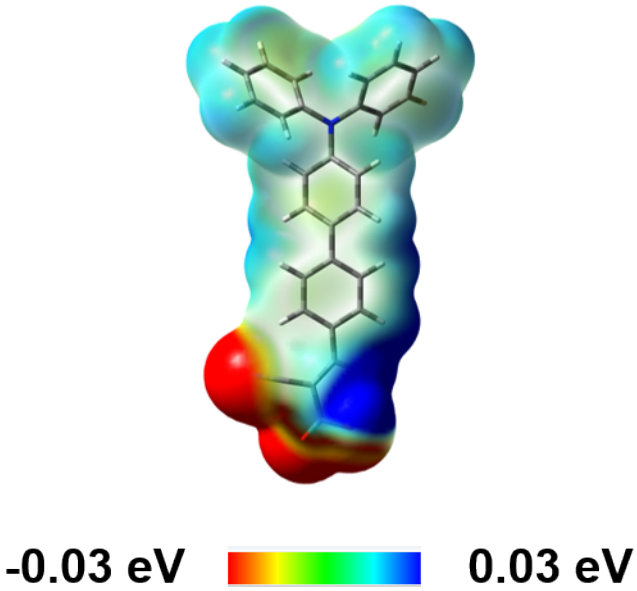

Figure S4. The ESP distribution of 2Cl-TPA-CN-COOH. The more negative electron distribution is attributed to the strong electron-withdrawing property of CN group. The positive is attributed to the electron-donating group of benzene ring.

Table S1. The thermal annealing temperature optimization details of 2Cl-TPA-CN-

COOH (0.3 mg/ml) for 5 min.

Annealing temperature	V_{oc} (V)	J_{sc} (mA cm^{-2})	FF (%)	PCE (%)	Ave. PCE[a]
80	0.854	27.1	76.1	17.6	17.1
100	0.853	27.5	79.6	18.6	18.3
120	0.849	27.0	78.1	17.7	17.3

a: The average PCE obtained from 10 devices

Table S2. The thermal annealing temperature optimization details of 2Cl-TPA-CN-COOH (0.3 mg/ml)

Concentration	V_{oc} (V)	J_{sc} (mA cm^{-2})	FF (%)	PCE (%)	Ave. PCE[a]
0.15	0.850	27.1	71.4	16.4	16.0
0.3	0.853	27.5	79.6	18.6	18.3
0.6	0.849	25.1	77.4	16.5	16.0

a: The average PCE obtained from 10 devices

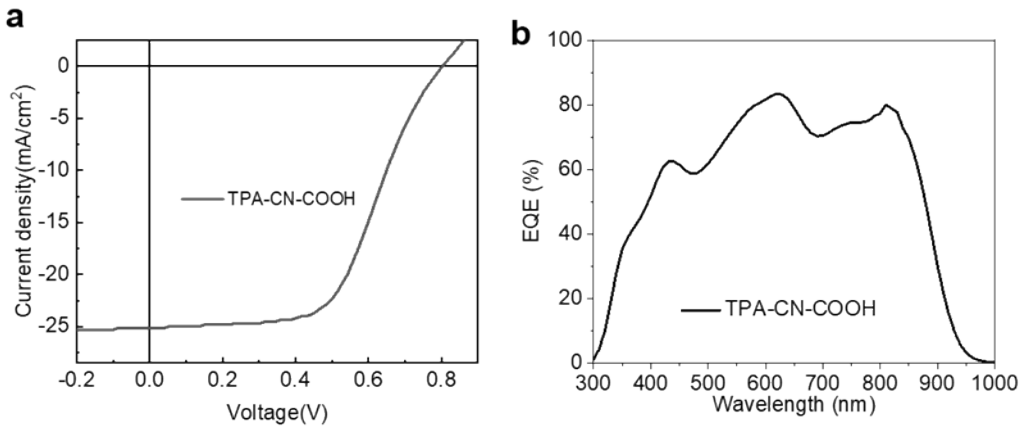

Figure S5. (a) The J-V curve based on TPA-CN-COOH self-assembling materials. The J_{sc}: 24.7 mA cm-2, V_{oc}: 0.78 V, FF:51.2%, PCE:10.0%. From these parameters, we can conclude that TPA-CN-COOH material is not suitable for the OSC field. (b) The EQE spectrum based on TPA-CN-COOH self-assembling materials.

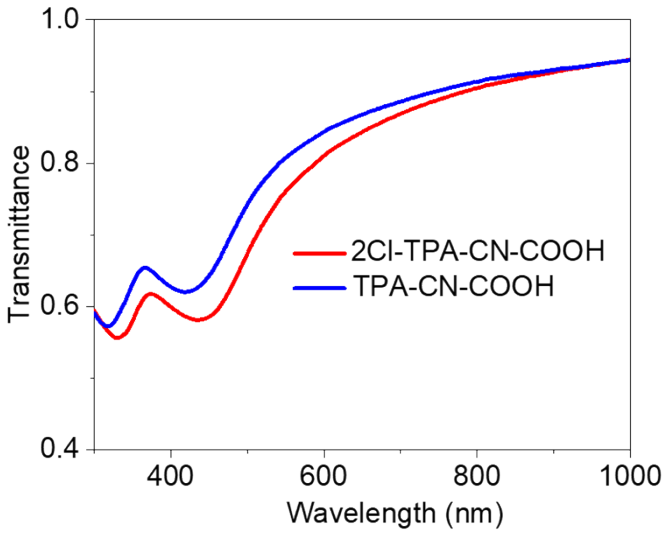

Figure S6. The transmittance of TPA-CN-COOH and 2Cl-TPA-CN-COOH film coated on quartz substrate.

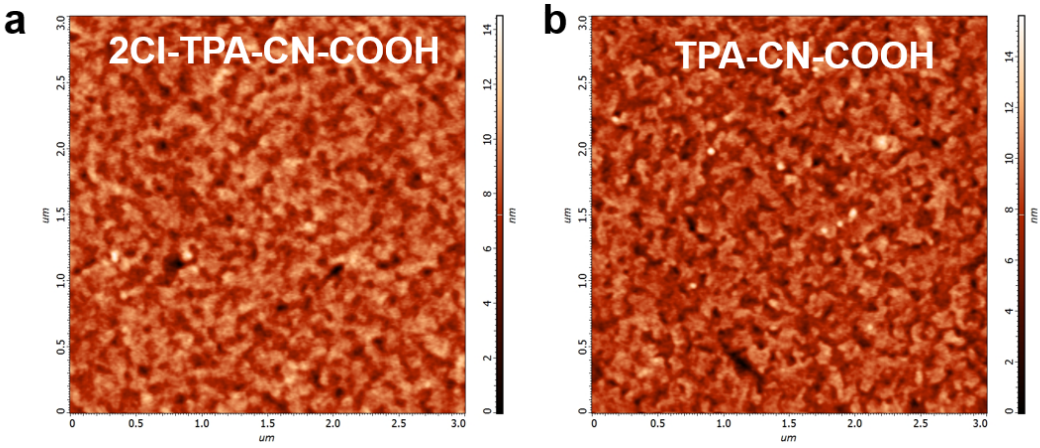

Figure S7. The surface morphology of TPA-CN-COOH (a) and 2Cl-TPA-CN-COOH (b) film tested by atomic force microscopy (AFM). The root-mean-square (RMS) value for TPA-CN-COOH and 2Cl-TPA-CN-COOH is 0.79 nm and 0.84 nm, respectively.

V_{oc} as a function of light intensity

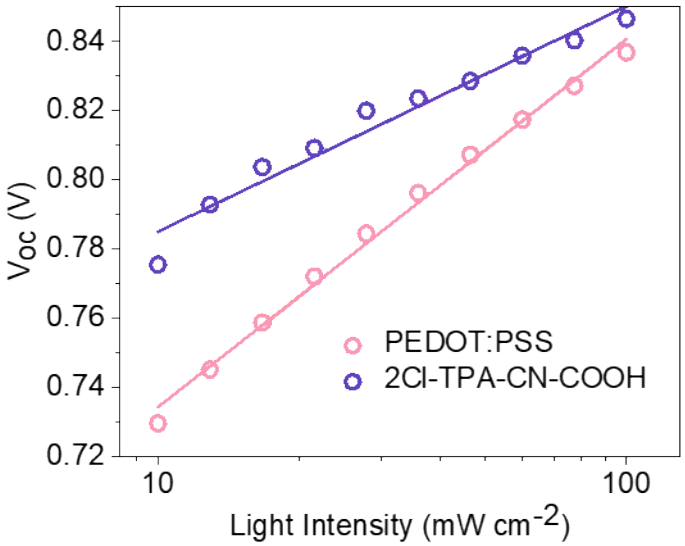

Figure S8. The plot of V_{oc} as a function of light intensity of PEDOT:PSS and 2Cl-TPA-CN-COOH based devices. The correlation between V_{oc} and I generally follows the equation: $V_{oc} \propto \ln(I) nkT/q$, where k, q and T are the Boltzmann constant, elementary charge and Kelvin temperature, respectively. The slope in the range from kT/q to 2 kT/q is applied to distinguish whether the charge carrier transport is constrained by the trap-assisted recombination.

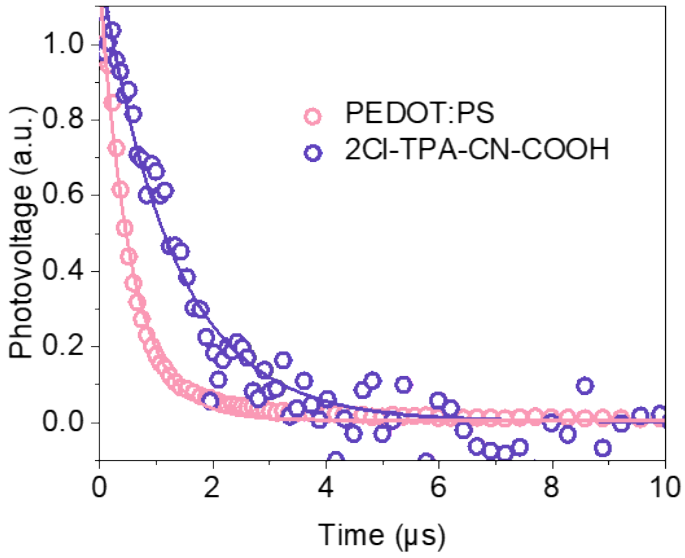

Figure S9. The TPV curves of PEDOT:PSS and 2Cl-TPA-CN-COOH based devices. Where the voltage is tracked by increasing the extraction time under the open-circuit condition.

Deep level transient spectroscopy (DLTS) Test

The transient current response is analyzed by applying a negative voltage of -3V to the device in the dark. Using the following equation to estimate the defect distributions in organic semiconductors. Considering the dependence of carrier transport position in the device, the current peak in the first 0.1μs is mainly caused by the displacement current, so the fitting of 0.1 ~ 100μs at room temperature are dominant. The trapped defect state volume density Nt of the discrete energy trap can be expressed as:

$$j_{te}(t) = \frac{1}{\tau_{te}} \cdot q \cdot d \cdot N_t \cdot exp(-\frac{t}{\tau_{te}})$$

Where $j_{te}(t)$ is trap emission current, τ_{te} is catch-trap emission time constant, q is a single charge amount, d is the film thickness of the device, N_t is the trap state density.

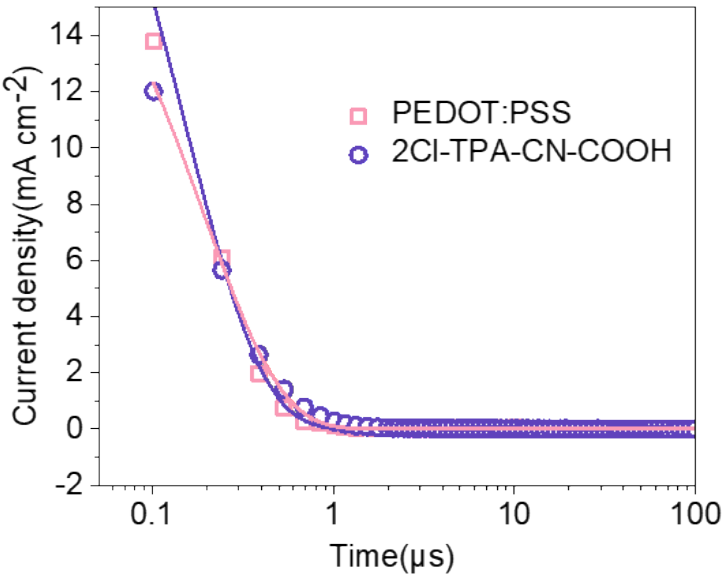

Figure S10. The DLTS curves of PEDOT:PSS and 2Cl-TPA-CN-COOH based devices. Then from this DLTS cruces, the trap density can be fitted according to the above equation.

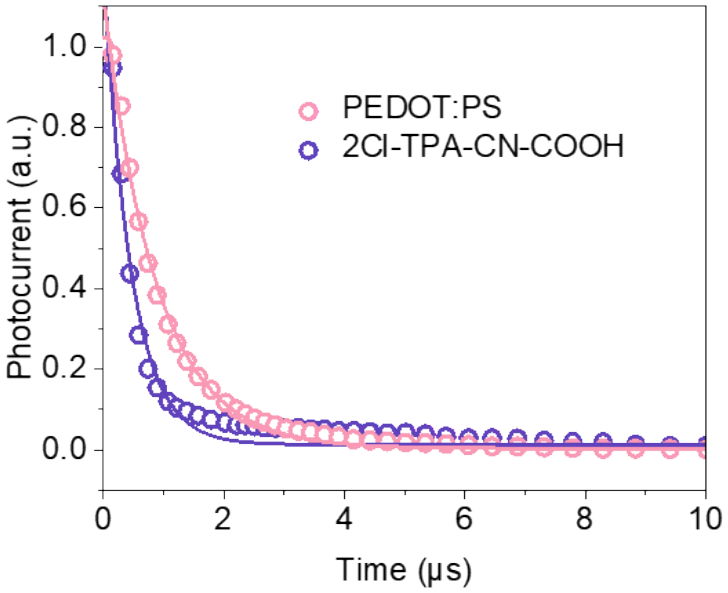

.

Figure S11. The TPC curves of PEDOT:PSS and 2Cl-TPA-CN-COOH based devices.

where the current is tracked by increasing the extraction time under the short-circuit condition.

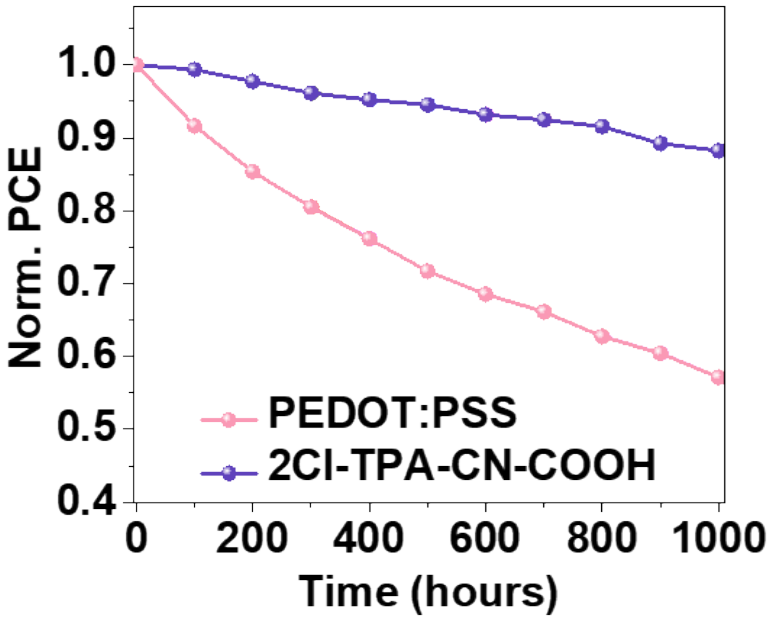

Figure S12. The shelf-lifetime performance degradation curves of PEDOT:PSS and 2Cl-TPA-CN-COOH based devices under the nitrogen-atmosphere glove box for 1000 hours.

Materials and Synthesis details of 2Cl-TPA-CN-COOH

Unless stated otherwise, all commercially available chemicals and solvents were used without further purification. Bis(4-chlorophenyl)amine purchased from Bide Pharmatech Co., Ltd. Compound TPA-CN-COOH were synthesized according previous report(*ACS Mater. Lett*, 2022, **4**, 1976-1983).

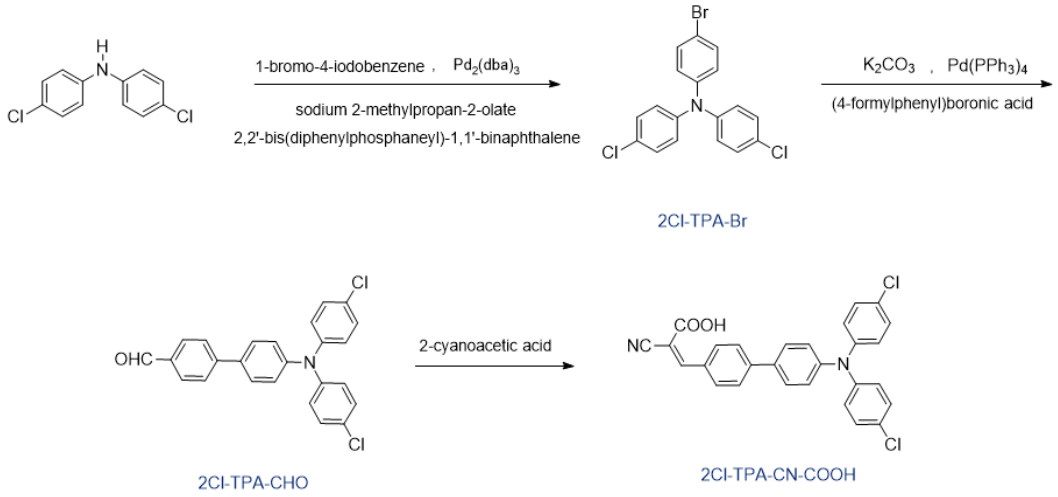

Figure S13. Synthetic route of 2Cl-TPA-CN-COOH

Synthesis of 2Cl-TPA-Br

A solution of *bis(4-chlorophenyl)amine* (650 mg, 2.73mmol), *1-bromo-4-iodobenzene* (850 mg, 3.00 mmol), *tris(dibenzylideneacetone)dipalladium(0)*Pd_2-$(dba)_3$) (75 mg, 0.082 mmol), *2,2'-bis(diphenylphosphaneyl)-1,1'-binaphthalene* (170 mg, 0.27 mmol) and *sodium-2-methylpropan-2-otate* (577 mg, 6.01 mmol) was purged with nitrogen. After refluxing at 115 ℃ overnight, the organic layer was extracted with ethyl acetate (3×100 mL) and washed with water for three times. The combined organic phase was dried over anhydrous $MgSO_4$. After solvent removal, the residue was purified using column chromatography on silica gel using petroleum ether/dichloromethane (5:1, V/V) as the eluent. The title compound was obtained as a white solid (0.82 g, 77 %). ^{1}H NMR (400 MHz, $CDCl_3$) δ 7.39-7.30 (m, 2H), 7.21 (td, *J* = 6.7, 2.2 Hz, 4H), 7.00 - 6.97 (m, 4H), 6.94-6.88 (m, 2H).

Synthesis of 2Cl-TPA-CHO

2Cl-TPA-Br (820 mg, 2.09 mmol), (*4-formylphenyl)boronic acid* (469 mg, 3.13 mmol), K_2CO_3 (2 M, 6.26 mL), $Pd(PPh_3)_4$ (241 mg, 0.21 mmol) and 25 mL of THF were sequentially added under argon protection, and the mixture were heated to 90 °C in an oil bath. The reaction was stirring under reflux overnight. After the reactant was cooled to room temperature, the organic layer was extracted with dichloromethane (3×100 mL) and washed with water for three times. The combined organic phase was dried over anhydrous $MgSO_4$. After solvent removal, the residue was purified using column chromatography on silica gel using petroleum ether/dichloromethane (2:1, V/V) as the eluent. The title compound was obtained as a yellow solid (653 mg, 75 %). ^{1}H NMR (400 MHz, $CDCl_3$) δ 10.07 (s, 1H), 7.96 (d, *J* = 8.1 Hz, 2H), 7.75 (d, *J* = 8.1 Hz, 2H), 7.57 (d, *J* = 8.5 Hz, 2H), 7.28 (d, *J* = 9.0 Hz, 4H), 7.15 (d, *J* = 8.5 Hz, 2H), 7.08 (d, *J* = 8.6 Hz, 4H). ^{13}C NMR (100 MHz, $CDCl_3$) δ 191.86, 147.59, 146.33, 145.65, 134.90, 133.93, 130.39, 129.64, 128.69, 128.34, 127.05, 125.72, 123.64. HRMS: ESI m/z calcd. for $C_{25}H_{17}Cl_2NO$, 417.0687; found, 417.0684.

Synthesis of 2Cl-TPA-CN-COOH

Under argon protection, *TPA-CHO* (240 mg, 0.574 mmol), *cyanoacetic acid* (195 mg, 2.29 mmol), *$CHCl_3$* (20 mL) and piperidine (0.15 mL) were added in a 50 mL round-

bottomed flask. The temperature was increased to 50 ℃, and the reflux reaction was maintained for 16 h. After the reactant was cooled to room temperature, the organic solvent was removed by rotary evaporation, the remaining solid was dissolved in dichloromethane, washed with water, and the organic phase was collected and dried with anhydrous sodium sulfate. After solvent removal, the residue was purified using column chromatography on silica gel using dichloromethane: methanol (2:1, *V*/*V*) as the eluent. The title compound was obtained as a orange solid (153 mg, 55 %). ^{1}H NMR (400 MHz, DMSO-d6) δ 8.04 (s, 1H), 7.98 (d, *J* = 8.1 Hz, 2H), 7.80 (d, *J* = 8.1 Hz, 2H), 7.72 (d, *J* = 8.4 Hz, 2H), 7.38 (d, *J* = 8.7 Hz, 4H), 7.08 (t, *J* = 7.3 Hz, 6H). ^{13}C NMR (101 MHz, DMSO-d6) δ 164.00, 160.04, 149.90, 146.72, 145.48, 142.33, 133.29, 131.04, 130.69, 129.69, 128.14, 127.43, 126.64, 125.76, 123.58, 118.10. HRMS: ESI m/z calcd. for $C_{28}H_{18}Cl_2N_2O_2Na$, $[M+Na]^+$ 507.0643; found, 507.0653.

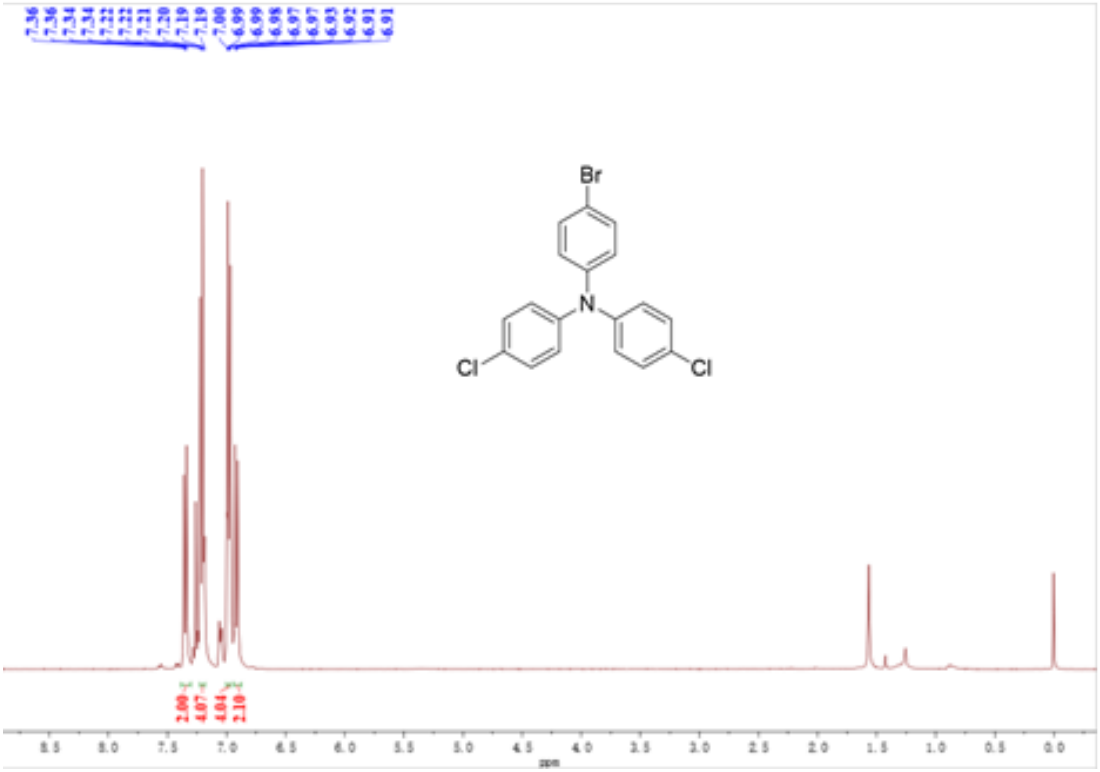

Figure S14. ^{1}H NMR spectrum of compound 2Cl-TPA-Br.

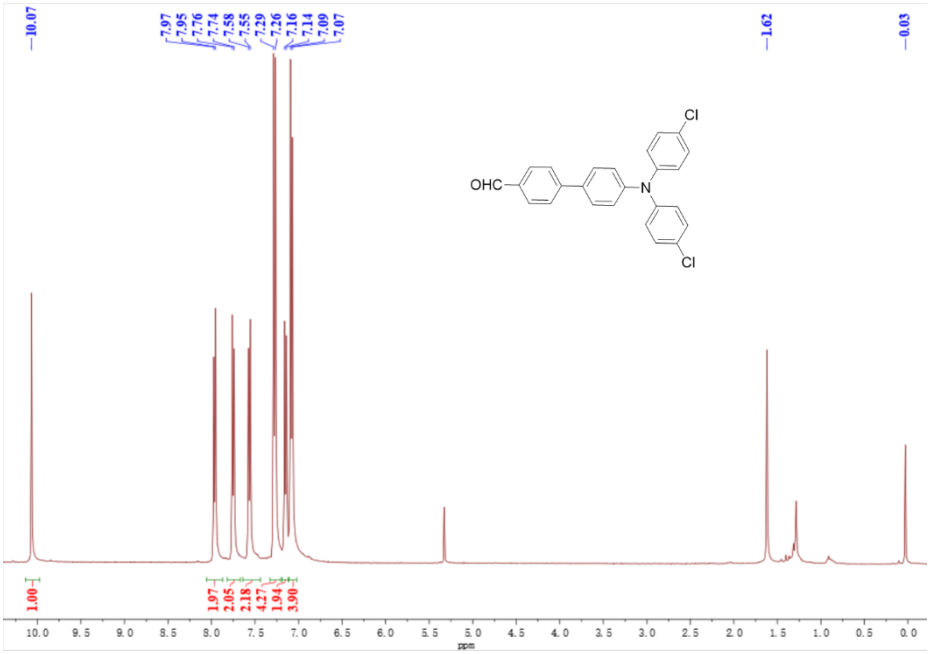

Figure S15. ^{1}H NMR spectroscopy of compound 2Cl-TPA-CHO.

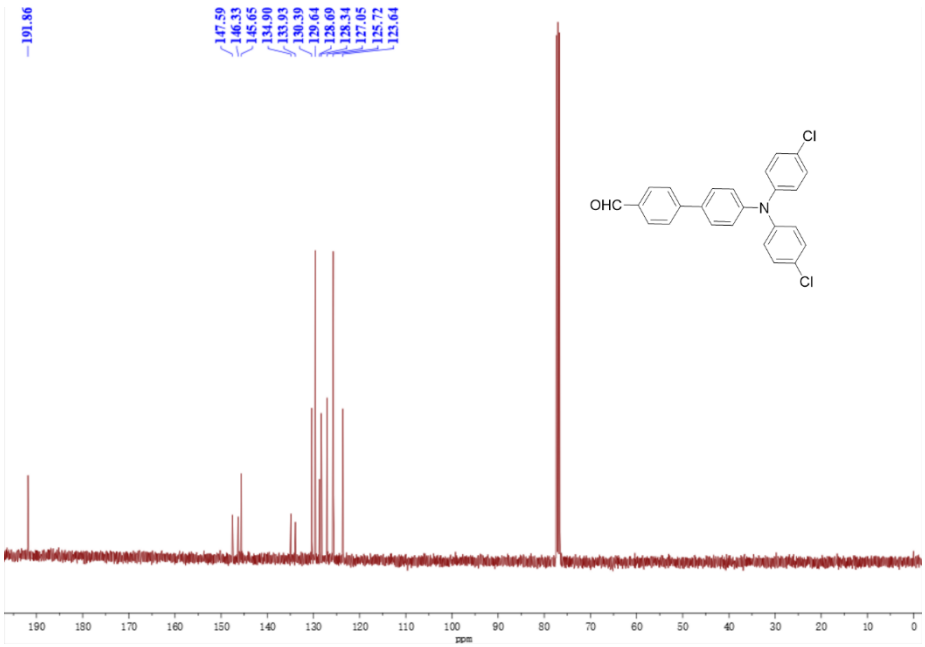

Figure S16. ^{13}C NMR spectroscopy of compound 2Cl-TPA-CHO.

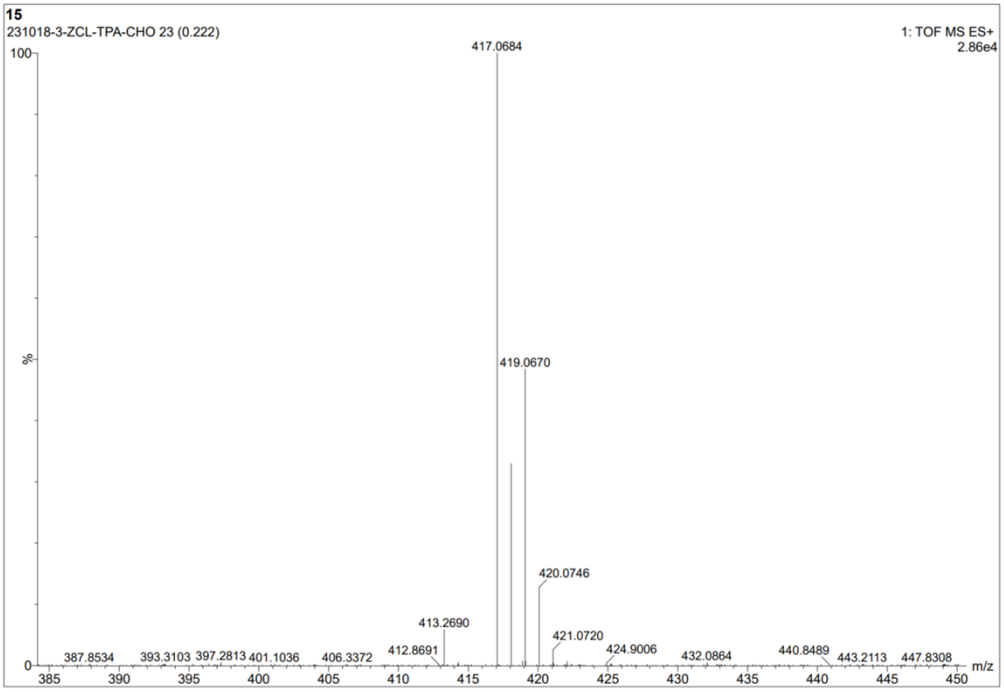

Figure S17. The TOF MS (ES+) plot of compound 2Cl-TPA-CHO.

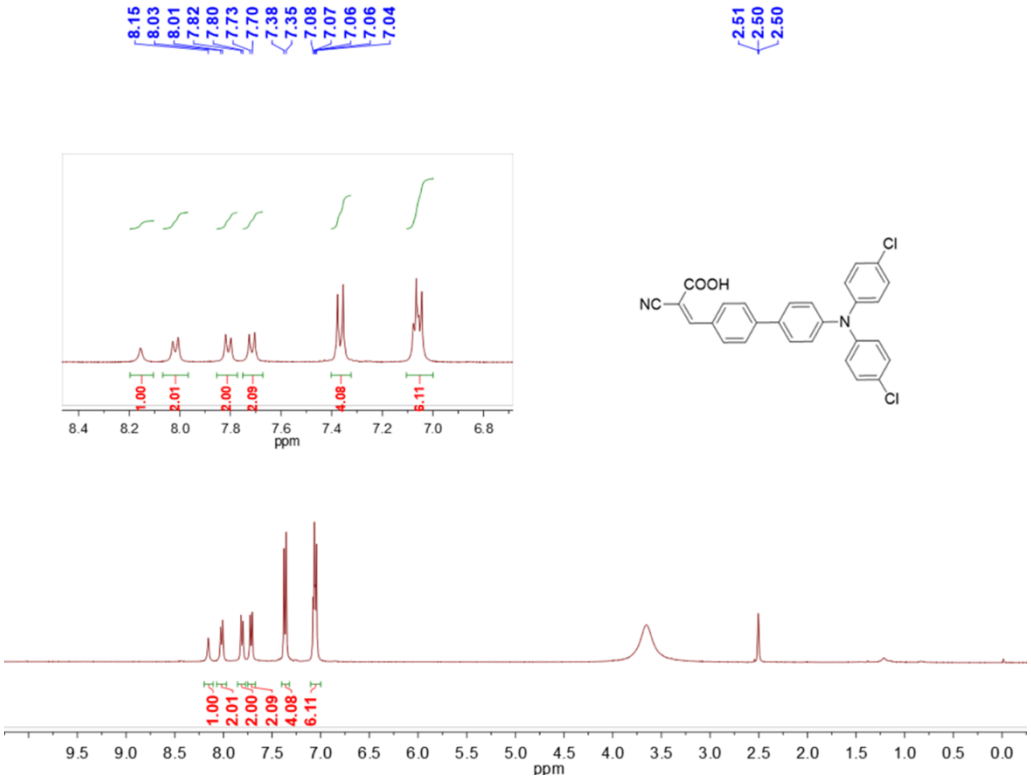

Figure S18. ^{1}H NMR spectroscopy of compound 2Cl-TPA-CN-COOH.

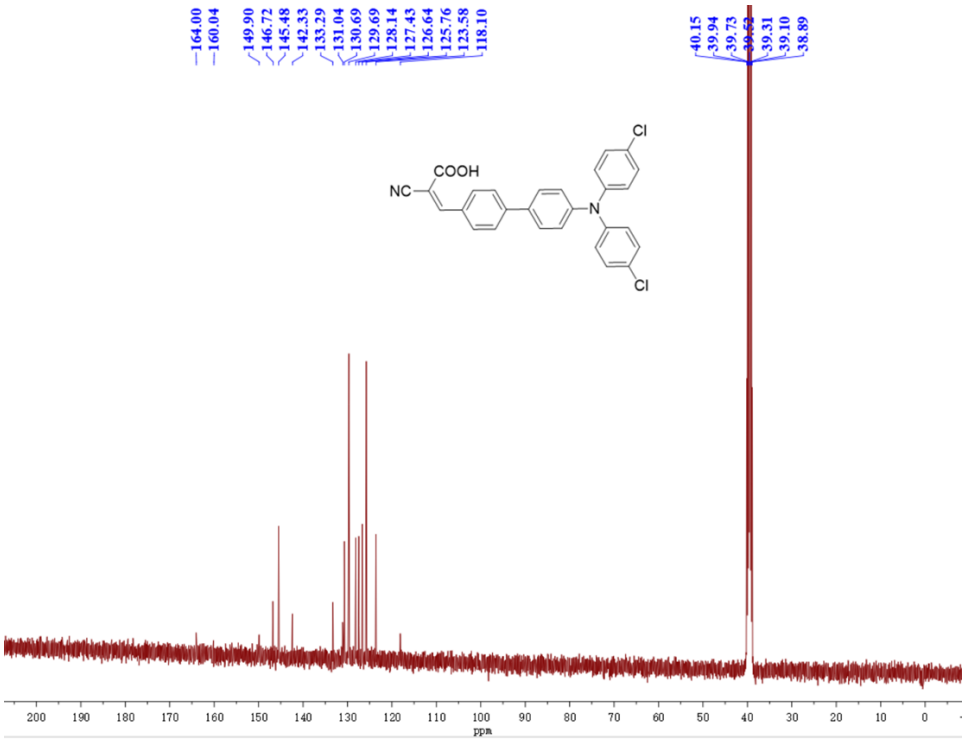

Figure S19. ^{13}C NMR spectroscopy of compound 2Cl-TPA-CN-COOH.

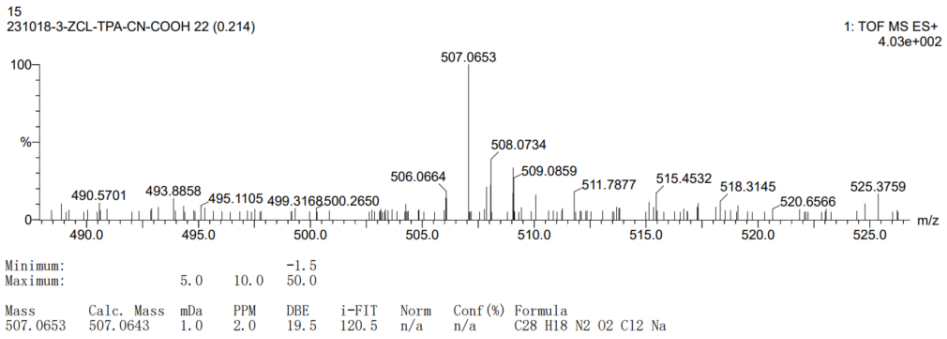

Figure S20. The TOF MS (ES+) plot of compound 2Cl-TPA-CN-COOH.